Conditional inactivation of *Fgfr1* in mouse defines its role in limb bud establishment, outgrowth and digit patterning

Jamie M. Verheyden[1], Mark Lewandoski[2], Chuxia Deng[3], Brian D. Harfe[4] and Xin Sun[1,*]

[1]Laboratory of Genetics, University of Wisconsin-Madison, 425G Henry Mall, Madison, WI 53706, USA
[2]Cancer and Developmental Biology Laboratory, National Cancer Institute, Frederick Cancer Research and Development Center, Frederick, MD 21702, USA
[3]Genetics of Development and Disease Branch, NIDDK, NIH, 10/9N105, 10 Center Drive, Bethesda, MD 20892, USA
[4]University of Florida College of Medicine, Department of Molecular Genetics and Microbiology, Gainesville, FL 32610-0266, USA
*Author for correspondence (e-mail: xsun@wisc.edu)

Accepted 18 July 2005

Development 132, 4235-4245
Published by The Company of Biologists 2005
doi:10.1242/dev.02001

Summary

Previous studies have implicated fibroblast growth factor receptor 1 (FGFR1) in limb development. However, the precise nature and complexity of its role have not been defined. Here, we dissect *Fgfr1* function in mouse limb by conditional inactivation of *Fgfr1* using two different Cre recombinase-expressing lines. Use of the *T* (brachyury)-cre line led to *Fgfr1* inactivation in all limb bud mesenchyme (LBM) cells during limb initiation. This mutant reveals FGFR1 function in two phases of limb development. In a nascent limb bud, FGFR1 promotes the length of the proximodistal (PD) axis while restricting the dimensions of the other two axes. It also serves an unexpected role in limiting LBM cell number in this early phase. Later on during limb outgrowth, FGFR1 is essential for the expansion of skeletal precursor population by maintaining cell survival. Use of mice carrying the sonic hedgehog^{cre} (*Shh*^{cre}) allele led to *Fgfr1* inactivation in posterior LBM cells. This mutant allows us to test the role of *Fgfr1* in gene expression regulation without disturbing limb bud growth. Our data show that during autopod patterning, FGFR1 influences digit number and identity, probably through cell-autonomous regulation of *Shh* expression. Our study of these two *Fgfr1* conditional mutants has elucidated the multiple roles of FGFR1 in limb bud establishment, growth and patterning.

Key words: Cre-mediated recombination, FGF, *Fgfr1* signaling, Limb development, Mouse, Patterning, *Shh*

Introduction

Mouse limbs initiate as limb buds that protrude from set positions along the side of the embryo. Early limb buds consist of an ectoderm-derived epithelial jacket encasing morphologically undifferentiated mesoderm-derived mesenchymal cells. Signaling between these two cell lineages is important for limb development along its three axes: the proximodistal (PD or shoulder to fingertip) axis, the anteroposterior (AP or thumb to little finger) axis and the dorsoventral (DV or back of hand to palm) axis (Niswander, 2003). In particular, the apical ectodermal ridge (AER), a specialized group of ectodermal cells that rims the growing tip of the limb bud, emits signals for the growth and patterning of the underlying mesenchyme. Key signals involved in this process are fibroblast growth factors (FGFs) and several Fgf genes are expressed in the AER (*AER-Fgfs*). Limb-specific inactivation of two *AER-Fgfs*, *Fgf4* and *Fgf8*, leads to severe reduction of skeletal elements in all three limb segments along the PD axis (Boulet et al., 2004; Sun et al., 2002). Analysis of these mutants led to the proposal that AER-FGFs are important for the expansion of the skeletal precursor population for each segment of the limb (Sun et al., 2002). The exact mechanism by which AER-FGFs direct cellular changes in the underlying mesenchyme is unclear.

There are four mouse FGF receptors (FGFRs), each characterized by three extracellular immunoglobulin (Ig)-like domains, a single transmembrane domain and an intracellular split cytoplasmic tyrosine kinase domain (Itoh and Ornitz, 2004). Alternative splicing within the third Ig loop of FGFR1-3 produces two splice variants: IIIb and IIIc which display different ligand specificities. For example, mitogenic assays in cultured cells show that FGF4 and FGF8 preferentially activate the IIIc isoform of FGFR (Ornitz et al., 1996). Conversely, genetic data suggest that FGF10, which is expressed in the LBM, preferentially activates the IIIb isoform (Min et al., 1998; Revest et al., 2001; Sekine et al., 1999). In addition, the IIIb and IIIc isoforms are often differentially expressed, with IIIb preferentially in the epithelium and IIIc in the mesenchyme (Finch et al., 1995; Orr-Urtreger et al., 1993; Peters et al., 1992).

Two Fgfrs, *Fgfr1* and *Fgfr2* are expressed in the early limb bud (Orr-Urtreger et al., 1993; Peters et al., 1992; Xu et al., 1998; Yamaguchi et al., 1992). *Fgfr2-IIIc*, although expressed in early LBM, is only essential at a later stage in ossification (Eswarakumar et al., 2002; Yu et al., 2003). A role for FGFR1 in limb has been implicated through studies of chimera and hypomorphic mutants, which bypass the gastrulation defect that causes *Fgfr1*$^{-/-}$ mutants to die prior to limb initiation (Ciruna and Rossant, 2001; Deng et al., 1994; Yamaguchi et

al., 1994). These milder mutants exhibit deformed limb buds and varying degrees of reduction in limb skeletal elements (Deng et al., 1997; Partanen et al., 1998; Xu et al., 1999). However, the precise role of FGFR1 in limb formation awaits definition. Here, we dissect FGFR1 function by conditional inactivation in mouse using the Cre/*loxP* approach. Our results show that FGFR1 plays multiple roles in limb bud establishment, outgrowth and patterning.

Materials and methods

Generation of *Fgfr1* limb mutants

Mice carrying a conditional allele of *Fgfr1* (*Fgfr1*^{co}) (Xu et al., 2002) were mated to either Tcre line (Perantoni et al., 2005) or *Shh*^{cre} (Harfe et al., 2004) allele to generate Tcre;*Fgfr1* and *Shhcre;Fgfr1* mutant embryos, respectively. Offspring were genotyped using the following PCR primer pairs: for Cre, 5′-TGATGAGGTTCGCAAGAACC-3′ and 5′-CCATGAGTGAACGAACCTGG-3′; for *Fgfr1*, 5′-CTGGTATCCTGTGCCTATC-3′ and 5′-CAATCTGATCCCAAGACCAC-3′.

RT-PCR analysis

For normal and *Tcre;Fgfr1* mutant limb buds (two pairs each), the LBM was dissected from the ectoderm and total RNA was prepared using TRIzol (Invitrogen). First-strand synthesis was carried out using the Superscript First Strand cDNA Synthesis Kit (Invitrogen). PCR was performed using the following primer pairs: for *Fgfr1*, 5′-TCTGGAAGCCCTGGAAGAGAGA-3′ and 5′-TCTTAGAGGCAAGATACTCCAT-3′; for *Gapdh*, 5′-ACCACAGTCCATGCCATCAC-3′ and 5′-TCCACCACCCTGTTGCTGTA-3′.

Embryo isolation and phenotype analyses

Embryos were dissected from time-mated mice, counting noon on the day the vaginal plug was found as embryonic day (E) 0.5. Whole-mount in situ hybridization was performed as previously described (Neubuser et al., 1997). The *Fgfr1* in situ probe was prepared from a plasmid containing *Fgfr1* exon 9 cDNA. This cDNA was generated by PCR using primer pair: 5′-TCTGGAAGCCCTGGAAGAGAGA-3′ and 5′-TGCGCAGAGGGATGCTCTTG-3′.

Limb buds for histological analysis were fixed in 4% paraformaldehyde after whole-mount in situ hybridization and embedded in JB-4 plastic resin (Polysciences) according to the manufacturer's protocol. Sections were cut at 5 μm and counterstained with 0.1% nuclear fast red. Skeletal preparations were performed with Alcian Blue and Alizarin Red using a standard protocol.

Areas of cell death were detected by staining with LysoTracker Red DND-99 (Molecular Probes) using a modified protocol (Zucker et al., 1999).

Shh-expressing cell lineage analysis

For lineage analysis, the Cre reporter line *R26R* (Soriano, 1999) was introduced into the mutant background to generate mutant *Shh*$^{cre/+}$;*Fgfr1*$^{co/co}$;*R26R*/+ and control *Shh*$^{cre/+}$;*Fgfr1*$^{co/+}$;*R26R*/+ embryos. In embryos of either genotype, *lacZ* is expressed in Cre-expressing cells and their progeny (*Shh*-expressing lineage). These cells are visualized by β-galactosidase (β-gal) staining using a standard protocol.

Results

Two Cre recombinase lines are used to inactivate *Fgfr1* in the LBM

By whole-mount RNA in situ hybridization, we found that *Fgfr1* is widely expressed in the lateral plate mesoderm (LPM), including the LBM prior to as well as after limb initiation (Fig. 1E; data not shown), in agreement with previous findings (Orr-Urtreger et al., 1991; Peters et al., 1992; Yamaguchi et al., 1992). To by-pass the gastrulation-stage lethality of *Fgfr1* null allele (Ciruna and Rossant, 2001; Deng et al., 1994; Yamaguchi et al., 1994), we inactivated *Fgfr1* using an existing *Fgfr1* conditional allele, *Fgfr1*^{co} (Xu et al., 2002). Upon Cre-mediated recombination of this allele, *Fgfr1* exons 8-14 are deleted, resulting in a null allele in which both the IIIb and IIIc isoforms are inactivated. We generated two *Fgfr1* mutants using two Cre-expressing lines, the Tcre transgenic line (Perantoni et al., 2005) and mice carrying the *Shh*^{cre} allele (Harfe et al., 2004). We found no difference in phenotype between cre;*Fgfr1*$^{null/co}$ or cre;*Fgfr1*$^{co/co}$, and we therefore refer to these genotypes as *Tcre;Fgfr1* or *Shhcre;Fgfr1*, depending on which Cre-expressing line was used. Tcre is generated through a transgenic approach using a 500 bp *T* (brachyury) promoter (Clements et al., 1996) driving Cre expression in the primitive streak-derived mesoderm lineages starting at E7.5 (Perantoni et al., 2005). By mating Tcre line to a cre activity reporter line *R26R* (Soriano, 1999), we found that at E8.5 and E10.0, Tcre is active in the LPM posterior to the heart, including the LBM (Fig. 1A-C). As a result of Tcre function, *Fgfr1* is completely inactivated in *Tcre;Fgfr1* LBM at E10.0, supported by data from RT-PCR (Fig. 1M) and whole-mount in situ hybridization analysis using a probe hybridizing to the deleted region of *Fgfr1* (Fig. 1E,F). To assess the impact on FGF signal reception, we assayed for the expression of genes regulated by FGFs, including sprouty (*Spry*) *2*, *Spry4* and *Mkp3* (*Dusp6* – Mouse Genome Informatics) (Eblaghie et al., 2003; Kawakami et al., 2003; Minowada et al., 1999). Their expression suggests that FGF signaling is markedly reduced, although not abolished, in the *Tcre;Fgfr1* limb buds (Fig. 1I,J and Fig. 3S,T and data not shown). The most likely candidate to act redundantly with *Fgfr1* to mediate this residual FGF signaling is *Fgfr2*. In *Tcre;Fgfr1* mutant limb buds, we found that *Fgfr2* is expressed normally compared with control (data not shown), and in accordance with previous published expression data (Orr-Urtreger et al., 1993; Xu et al., 1998).

Using the same analysis, in *Shhcre;Fgfr1*, we can detect a domain lacking *Fgfr1* expression in the posterior mesenchyme of E10.5 limb buds, shortly after the commencement of *Shh*^{cre} activity (Fig. 1D,G,H). *Spry4* and *Mkp3* gene expression is reduced in this domain (Fig. 1K,L and Fig. 5G,H).

Inactivating *Fgfr1* in LBM affects the size and shape of all three limb skeletal segments

Tcre;Fgfr1 mutants die at birth probably owing to neural tube and axial skeletal defects (see below). In E17.5 mutant forelimbs (n=8), we found that the stylopod is shortened by an average of 15%. The zeugopod, reduced by 12%, is often fused at the distal end (Fig. 2A,B, n=4/8 mutant forelimbs). The mutant autopod often consists of three digits, one tri-phalangeal digit flanked by two bi-phalangeal digits (Fig. 2E,F, n=5/8 forelimbs).

The *Tcre;Fgfr1* mutant hindlimb is more severely affected than the forelimb (Fig. 2C,D,G,H). One explanation for the increased severity is based on a possible reduction of LPM cell number in the prospective hindlimb, but not forelimb region prior to limb initiation. This reduction is deduced from a combination of phenotypes, including irregular somite size and

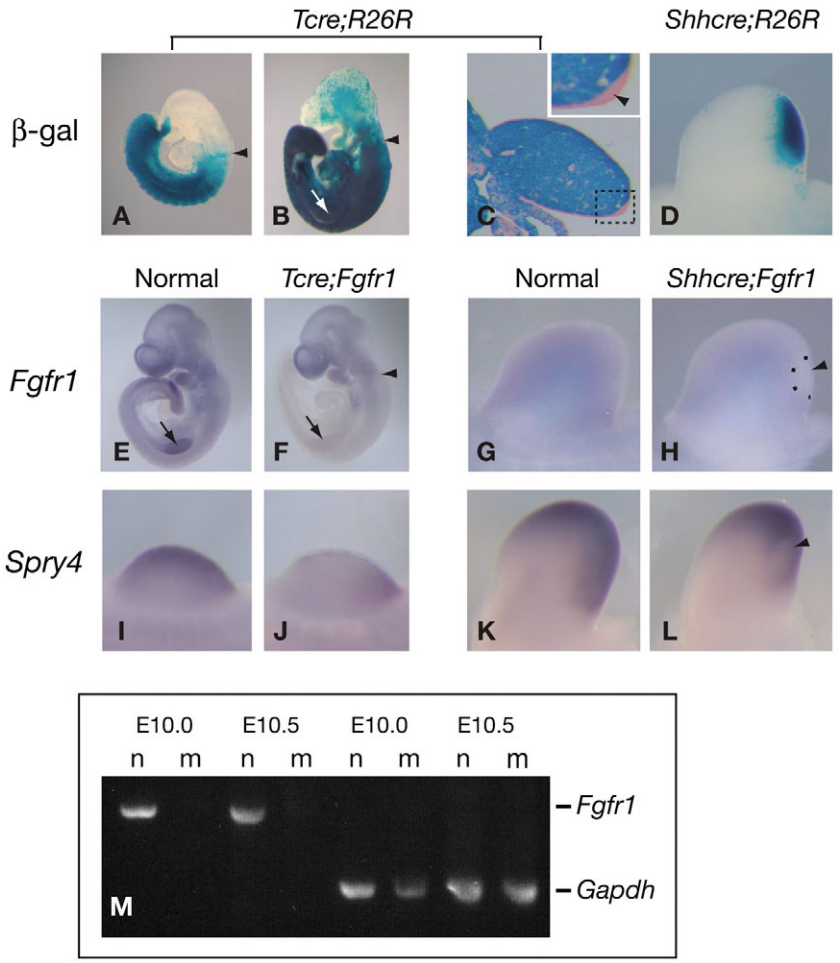

Fig. 1. Inactivation of *Fgfr1* by Tcre and *Shh*^{cre}. (A-D) β-Gal staining of embryos at E8.5 (A) and E10.0 (B), an E10.0 forelimb bud in transverse section (C) and an E10.5 intact limb bud (D). The arrowheads in A and B delineate the rostral boundary of robust staining. Arrow in B indicates the forelimb bud. Inset in C is a magnified view of the boxed domain to illustrate that the staining is robust in the mesenchyme, while absent in the AER (arrowhead). (E-L) Gene expression analysis using whole-mount in situ hybridization probes indicated on the left. (E,F) E10.0 embryos. Arrows in E,F indicate forelimb buds. Arrowhead in F delineates the rostral boundary of *Fgfr1* inactivation. (G,H) E10.5 forelimb buds. Broken line and arrowhead in H indicate *Fgfr1* inactivation in posterior mesenchyme. (I,J) E10.0 forelimb buds. Expression of *Spry4* in the mutant is reduced to the posterior mesenchyme and a thin line subjacent to the AER. (K,L) Oblique dorsoposterior view of E10.5 forelimb buds. Arrowhead in L indicates reduced *Spry4* expression in the dorsoposterior mesenchyme. (M) RT-PCR of normal (n) and *Tcre;Fgfr1* mutant (m) limb buds to illustrate that *Fgfr1* is inactivated in mutant LBM at E10.0 and E10.5.

an expanded open neural plate at E9.5, and misshapen ribs and axial vertebrae at E17.5 (data not shown). These defects are probably due to a previously described requirement of *Fgfr1* in mesoderm production (Ciruna and Rossant, 2001; Ciruna et al., 1997; Deng et al., 1997; Yamaguchi et al., 1994). In *Tcre;Fgfr1* hindlimb, a defect in mesoderm production will lead to reduced prospective LBM cell number, and in turn a reduced limb skeleton. By contrast, none of the phenotypes indicative of mesoderm reduction is observed within and rostral to the forelimb region, suggesting that the phenotypes observed in the forelimb are not compounded by earlier defects in mesoderm production. Thus, to address the specific role of FGFR1 in limb development, we have concentrated on the forelimb of the *Tcre;Fgfr1* mutant for subsequent analyses.

Using *Sox9* expression to outline the initial cartilage condensations, we found that a reduction in condensation size and number contributes to reduced forelimb skeletons in the *Tcre;Fgfr1* mutant (Fig. 2I-L). In addition, we found that at E11.5, although five distinct condensations are observed in wild-type forelimb buds (Fig. 2I, *n*=4 limb buds), individual condensations cannot be discerned in the *Tcre;Fgfr1* forelimb buds (Fig. 2J, *n*=4 limb buds). This suggests that separation of the digit condensations is delayed in *Tcre;Fgfr1* mutant.

Based on phalanx number, the two bi-phalangeal digits in the *Tcre;Fgfr1* forelimb might be of digit 1 character. To address whether this conclusion is also supported by molecular characteristics, we assayed for *Hoxd12* and *Hoxd13* expression (Fig. 2M-P). Previous studies show that digit 1 identity is marked by the absence of *Hoxd12* and presence of *Hoxd13* expression (Fromental-Ramain et al., 1996; Knezevic et al., 1997; Zakany et al., 1997). Their expression in *Tcre;Fgfr1* mutant limb buds supports that the most anterior digit is digit 1, while the most posterior digit is not, despite being biphalangeal. These results show that in *Tcre;Fgfr1* limbs, digit 1 is present while some of the posterior digits are absent.

Fgfr1 regulates nascent limb bud shape and cell number

We found that the *Tcre;Fgfr1* forelimb bud is misshapen at E10.0 shortly after limb initiation. Although shorter along the PD axis, it is wider along the AP axis and thicker along the DV axis (Fig. 3A,B,E,F). By E10.5, the differences in all three axes are further exaggerated (Fig. 3C,D,G,H). A previous study of *Fgfr1* hypomorphic mutants show that a posterior shift in *Hoxb9* expression in the LPM may be responsible for the expansion of limb bud AP width (Partanen et al., 1998). A careful examination of *Hoxb9* expression in *Tcre;Fgfr1* LPM shows that there is no posterior shift of expression in this mutant to explain the increase in width (data not shown).

Using *Fgf8* expression as a marker for AER, we found that in *Tcre;Fgfr1* forelimb buds the AER is wider along DV axis starting at E10.0 (Fig. 3I-L) and shorter along AP axis starting

at E10.5 (Fig. 3C,D). This suggests that *Fgfr1* inactivation in the mesenchyme can influence AER morphology in a cell non-autonomous manner. A possible mediator for this function is GREMLIN, a secreted antagonist of BMP signaling. *Gremlin* null mutants show a similar AER phenotype (Khokha et al., 2003; Michos et al., 2004), and its expression is downregulated in *Tcre;Fgfr1* limb buds (Fig. 3M,N).

To address whether the whole limb bud shape change is accompanied by cell number changes, we counted LBM cell number (see Table S1 in the supplementary material). Our result shows that there is an approximate increase of 65% and 31% in the number of cells in the *Tcre;Fgfr1* forelimb buds compared with controls at E10.0 and E10.5, respectively. At these stages, using phosphorylated Histone H3 antibody staining, no significant difference in cell proliferation is detected between mutant and normal to account for the increase in cell number (data not shown).

The initial excess cell number in *Tcre;Fgfr1* limb buds is quickly negated by increased cell death observed starting at E10.5 (Fig. 3O,P). By E11.5, a mutant limb bud on average has 26% fewer cells compared with normal (see Table S1 in the supplementary material). We found that the expression of *Dkk1*, a mediator of limb bud cell death (Grotewold and Ruther, 2002; Mukhopadhyay et al., 2001), is increased in *Tcre;Fgfr1* limb buds (Fig. 3Q,R). This provides a possible molecular mechanism for the cell death phenotype. Despite the increased number of dying cells, the death domain in *Tcre;Fgfr1* limb buds is confined to the proximal and anterior LBM, similar to normal (Fig. 3O,P). We hypothesize that no cell death is detected in the distal mesenchyme because these cells are protected by residual FGF signaling, as indicated by *Spry4* expression (Fig. 3S,T).

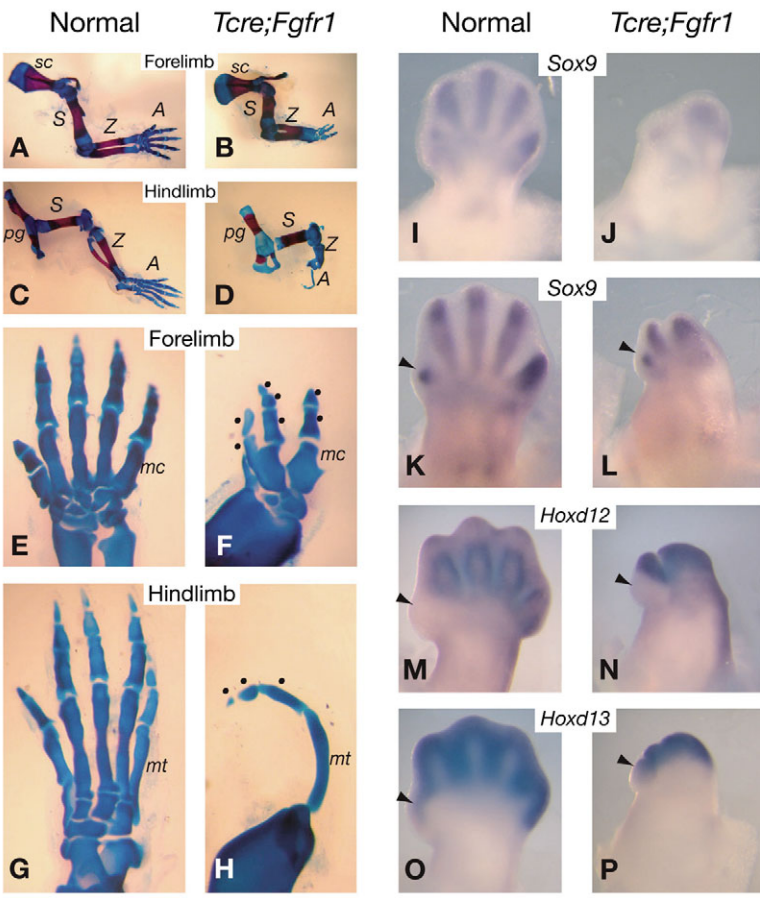

Fig. 2. *Tcre;Fgfr1* skeletal phenotypes and gene expression. (A-H) Skeletal preparations of E17.5 limbs, stained for cartilage (Alcian Blue) and bone (Alizarin Red). (A-D) All segments of the limb, the stylopod (*S*), zeugopod (*Z*) and autopod (*A*) are reduced in the mutant, while the structures outside of the limb, the scapula (*sc*) and pelvic girdle (*pg*), remain normal. (E-H) Magnified views of autopod skeletons. The positions of metacarpals (*mc*) and metatarsals (*mt*) are indicated. Dots in F and H indicate individual phalange. (I-P) Forelimb buds at E11.5 (I,J) and E12.5 (K-P). Arrowheads in K-P indicate the position of the most anterior digit.

Complete inactivation of *Fgfr1* in LBM affects the expression of key patterning genes

In search of additional molecular changes, we found that the expression of *Shh* is reduced to a very small domain in *Tcre;Fgfr1* forelimb buds (Fig. 4A,B). Accordingly, *Ptch1* and *Gli1* expression, which is responsive to the SHH signal, is detected in reduced domains (data not shown). In addition, *Alx4* expression, which is restricted by SHH signal to the anterior mesenchyme (Takahashi et al., 1998), is detected in a larger domain in the mutant (Fig. 4C,D). These results indicate that SHH signaling is reduced in the absence of FGFR1. The AER expression of all three BMP genes implicated in limb bud patterning, *Bmp2*, *Bmp4* and *Bmp7* is slightly upregulated in intensity in *Tcre;Fgfr1* limb buds, possibly owing to the widened AER (Fig. 4E-H; data not shown). Interestingly, the mesenchymal expression of *Bmp4* and *Bmp7* is slightly reduced, while that of *Bmp2* is upregulated in the *Tcre;Fgfr1* limb buds. This suggests that FGFR1 regulates Bmp gene expression in a complex manner.

A previous study of a hypomorphic *Fgfr1* mutant shows that *Hoxd13* expression is downregulated in those limbs (Partanen et al., 1998). Consistent with this, we found that in E10.5 *Tcre;Fgfr1* limb buds, expression of both *Hoxd13* and the paralogous *Hoxa13* is reduced, with *Hoxa13* more severely downregulated (Fig. 4I-L). Interestingly, by E12.5 *Hoxd13* expression in *Tcre;Fgfr1* limb buds appears to have recovered (compare Fig. 2P with Fig. 4L). A plausible explanation for this change is that early phase and late phase *Hoxd13* expression may be differentially controlled. This was also exemplified by a previous observation that in a limb-specific *Shh* chick mutant termed *oligozeugodactly* (*ozd*), early phase *Hoxd13* expression is absent while late phase expression is present (Ros et al., 2003). In summary, our molecular data suggest that a combination of these gene expression changes may account for the phenotypes in the *Tcre;Fgfr1* mutant.

Shhcre;Fgfr1 limb buds permit investigation of gene expression in the absence of growth defects

The downregulation of *Shh* expression in *Tcre;Fgfr1* limb buds supports the hypothesis of a transcriptional feedback loop between Fgf genes and *Shh* (Laufer et al., 1994; Niswander et

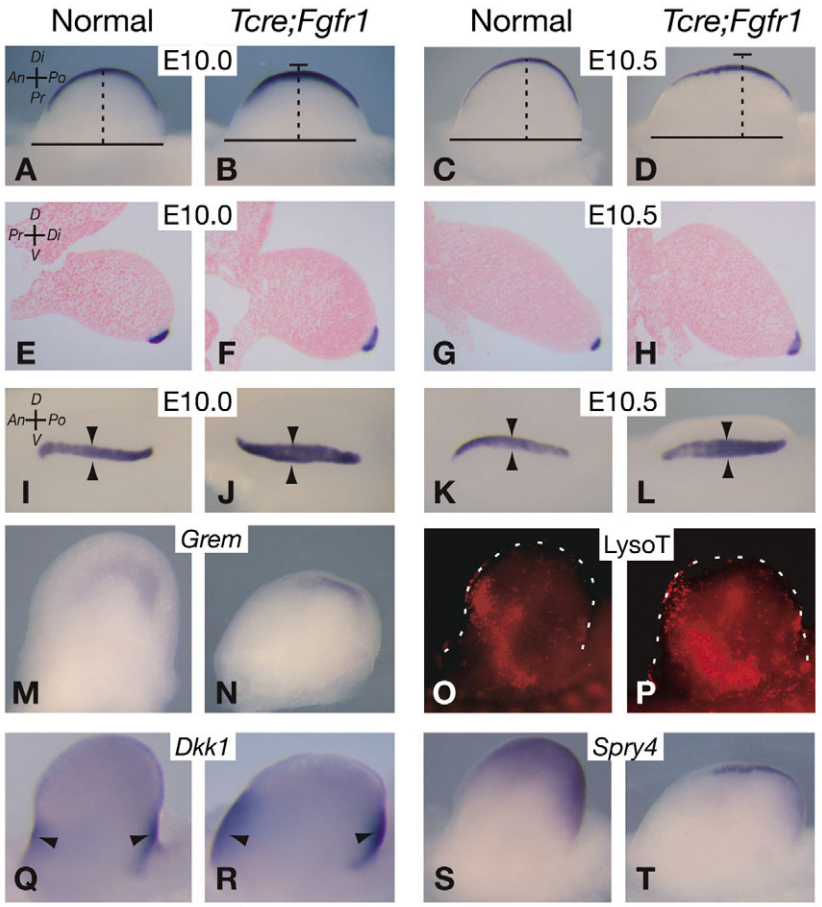

Fig. 3. *Tcre;Fgfr1* limb bud morphology and cell survival. (A-L) Forelimb buds at the indicated stages with the AER labeled by *Fgf8* whole-mount in situ hybridization. Each normal versus mutant pair is shown at the same magnification. (A-D) Dorsal view with the remaining axes indicated in A. Corresponding solid and broken lines in each pair are of the same length to assist comparisons of limb bud dimensions. (E-H) Transverse sections of limb buds. The mutant is thicker along the DV axis at E10.0 and E10.5. (I-L) Distal view with the remaining axes indicated in I. Arrowheads indicate that the mutant AER is wider than normal along the DV axis at E10.0 and E10.5. (M,N,Q-T) Gene expression, as indicated, in E10.5 forelimb buds as assayed by whole-mount in situ hybridization. Arrowheads in Q and R indicate expression in the mesenchyme. (O,P) Cell death in E10.5 forelimb buds assayed by LysoTracker Red staining. Limb buds are outlined by broken white lines. Abbreviations: *An*, anterior; *D*, dorsal; *Di*, distal; *Po*, posterior; *Pr*, proximal; *V*, ventral.

al., 1994). However, as the *Tcre;Fgfr1* and all of the previously characterized *AER-Fgf* mutant limb buds are abnormal in size and shape (Boulet et al., 2004; Sun et al., 2002), it remains possible that any detected reduction or absence of gene expression is due to changes in cell number.

The *Shhcre;Fgfr1* mutant offers several features essential for a rigorous test of FGFR1 function in gene expression regulation. First, this mutant presents a time window in which FGFR1 function in growth does not interfere with interpretation of data on gene expression. In *Shhcre;Fgfr1* limb buds, total limb bud size as well as size of the $Fgfr1^{-/-}$ domain as outlined by Shh^{cre} activity remains normal until E11.5 (Fig. 5A,B; data not shown). In addition, LysoTracker analysis indicates that there is no aberrant cell death at E10.75 and E11.5 (data not shown). These results suggest that in *Shhcre;Fgfr1* limb buds younger than E11.5, $Fgfr1^{-/-}$ cells are normal in number and capable of appropriate gene expression. Second, the *Shhcre;Fgfr1* mutant provides data on possible cell autonomous nature of gene expression regulation by FGFR1. In each *Shhcre;Fgfr1* limb bud, *Fgfr1* inactivation occurs in a cohort of cells within a clear boundary defined by the absence of *Fgfr1* or a reduction of *Spry4* and *Mkp3* expression (Fig. 1L, Fig. 5H). A gene expression change confined within $Fgfr1^{-/-}$ cells will support that FGFR1 regulates this gene cell-autonomously. Third, direct comparison of gene expression between $Fgfr1^{-/-}$ and normal cells within the same limb bud has increased our ability to detect subtle changes.

To address expression regulation in the context of *Shhcre;Fgfr1* limb buds, we first established $Shh^{cre/+};Fgfr1^{co/+}$ limb buds as a proper control. This is important because Shh^{cre} is generated by insertion of Cre into the *Shh*-coding region. Thus, only one wild-type copy of *Shh* remains in *Shhcre;Fgfr1* ($Shh^{cre/+};Fgfr1^{co/co}$) mutants. We found that the $Shh^{cre/+};Fgfr1^{co/+}$ control limb buds at E10.75 show robust *Shh* expression, despite having only one wild-type *Shh* allele and one wild-type *Fgfr1* allele (Fig. 5C). By contrast, in E10.75 *Shhcre;Fgfr1* mutant limb buds, *Shh* expression is reduced to a punctate pattern (Fig. 5D), demonstrating that *Fgfr1* cell-autonomously regulates *Shh* expression at the RNA level.

We noted that *Shh* expression is more reduced distally than proximally (asterisk in Fig. 5D). There is evidence that in a normal limb bud, endogenous *Shh* is expressed at a higher level distally than proximally (Dr Cliff Tabin, personal communication). Based on this, we favor the explanation that in *Shhcre;Fgfr1* limb buds, the PD difference in *Shh* inactivation is a result of differential *Shhcre* activity, and hence differential *Fgfr1* inactivation. Consistent with this, the expression patterns of *Fgfr1* and *Mkp3* at E10.75 (Fig. 5G,H; data not shown) indicate that FGF signal reception is efficiently reduced in the distal two-thirds, while it remains in the proximal one-third of the Shh^{cre} active domain (compare Fig. 5H with 5B). At later stages, *Shh* expression is progressively more reduced in *Shhcre;Fgfr1* limb buds, and eventually absent at E11.25, a time when it is still expressed in control limb buds (data not shown). To investigate factors that may mediate *Fgfr1* regulation of *Shh*, we examined *Hand2* (previously known as *dHAND*) expression, as it is necessary and sufficient to induce *Shh* expression (Charite et al., 2000). *Hand2* expression does not change in *Shhcre;Fgfr1* limb buds (data not shown), suggesting that HAND2 may act upstream of FGFR1, or that FGFR1 and HAND2 regulate *Shh* expression in parallel pathways.

As an example of non-cell-autonomous regulation, reduction of *Ptch1* expression is not restricted to the $Fgfr1^{-/-}$ domain, consistent with the idea that FGFR1 regulates *Ptch1* expression

through secreted SHH (Fig. 5E,F). Previous studies show that *Fgf10* expression in the mesenchyme is dependent on AER-FGF signaling (Boulet et al., 2004; Ohuchi et al., 1997). However, *Fgf10* expression is unaltered in *Shhcre;Fgfr1* limb buds (data not shown), suggesting that FGFR1 is not essential for *Fgf10* expression. Of the three Bmp genes investigated above, *Bmp2* expression remains normal, while *Bmp4* and *Bmp7* expression is reduced only within $Fgfr1^{-/-}$ cells, suggesting cell-autonomous regulation (Fig. 5I,J; data not shown).

The utility of *Shhcre;Fgfr1* mutant limb buds in gene expression studies is best demonstrated by data on *Hoxa13* and *Hoxd13*. In E11.5 *Shhcre;Fgfr1* limb buds, we consistently detected reduced *Hoxd13* expression in a wedge of cells in the anterior region of the $Fgfr1^{-/-}$ domain (n=5/5) (Fig. 5K,L). This suggests that FGFR1 cell-autonomously regulates the expression of *Hoxd13*, and that in the posterior $Fgfr1^{-/-}$ domain, its function may be redundant with other regulators of *Hox* expression. Interestingly, the expression of *Hoxa13* is unaltered in *Shhcre;Fgfr1* limb buds (data not shown), in contrast to our finding in *Tcre;Fgfr1* limb buds. These data together demonstrate that the analysis of *Shhcre;Fgfr1* limb buds has led to novel findings in FGF regulation of gene expression.

Inactivating *Fgfr1* in the *Shh*-expressing domain leads to absence of one digit

In all forelimbs and hindlimbs of *Shhcre;Fgfr1* mutants examined at E18.5 (n=6 embryos), the stylopod and zeugopod are normal in size, but the autopod is missing one digit (Fig. 6). Control ($Shh^{cre/+}$;$Fgfr1^{co/+}$) limbs display a normal skeletal pattern, suggesting that the phenotype we observed in the mutant is not a result of loss of a single allele of *Shh* and *Fgfr1*.

The absence of a digit could be due to reduced growth or a defect in AP patterning. We uncovered evidence to support the latter hypothesis. In E11.5 *Shhcre;Fgfr1* hindlimb buds, while limb bud size remains normal, only four condensations are detected by *Sox9* expression (Fig. 7A,B). Compared with wild type, the two middle condensations in the mutant are each wider and farther apart than any of the wild-type digit pairs. The differences are more pronounced in E11.5 forelimb buds (Fig. 7C,D). These observations suggest that when starting with a mesenchymal field of equivalent size, the presence or absence of FGFR1 function can lead to a difference in the number of digits placed.

It is interesting that in *Shhcre;Fgfr1* mutant only one digit is affected, as Shh^{cre} is capable of inactivating target gene function in prospective digits 4, 5 and part of digit 3 (Harfe et al., 2004). Although limited by lack of digit-specific molecular markers, both condensation as well as skeletal pattern data support the conclusion that digit 3 is absent. In an E11.5 wild-type forelimb bud, each of the condensations exhibits a characteristic morphology

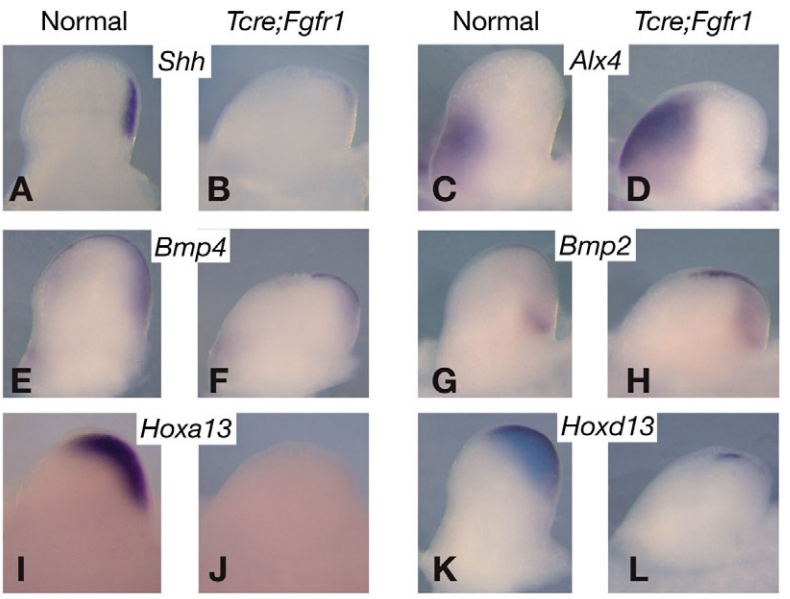

Fig. 4. Whole-mount in situ hybridization analysis of gene expression in *Tcre;Fgfr1* E10.5 forelimb buds. The mesenchymal expression of *Shh*, gremlin (*Grem*), *Bmp4*, *Hoxa13* and *Hoxd13* is reduced in the mutant, while the mesenchymal expression of *Alx4* and *Bmp2* and the AER expression of *Bmp4* and *Bmp2* is increased in the mutant.

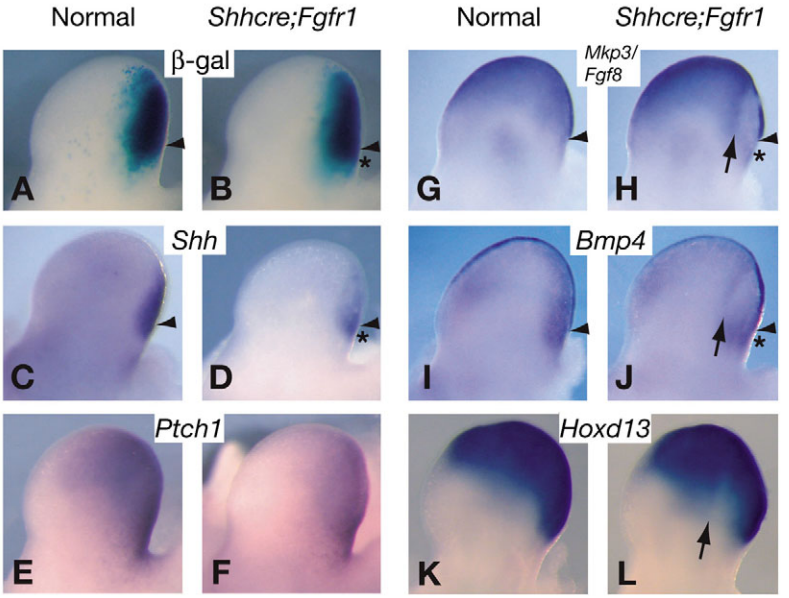

Fig. 5. Gene expression in *Shhcre;Fgfr1* limb buds. (A,B) β-Gal staining in (A) a $Shh^{cre/+}$;$Fgfr1^{co/+}$;*R26R*/+ and (B) a $Shh^{cre/+}$;$Fgfr1^{co/co}$;*R26R*/+ littermate E10.75 forelimb bud to label cells in which CRE has acted. (C-L) Gene expression in E10.75 (C-J) and (K,L) E11.5 forelimb buds. $Shh^{cre/+}$;$Fgfr1^{co/+}$ limb buds are used as normal control. Expression of *Shh*, *Mkp3*, *Bmp4* and *Hoxd13* is reduced within the CRE-active domain, while *Ptch1* is reduced outside of the domain. Arrowheads indicate the posterior end of the AER. Asterisks indicate signal in the mesenchyme proximal to the end of the AER. Arrows indicate that the anterior boundaries of *Bmp4* and *Hoxd13* reduction corresponds to that of *Fgfr1* inactivation as reported by *Mkp3* reduction.

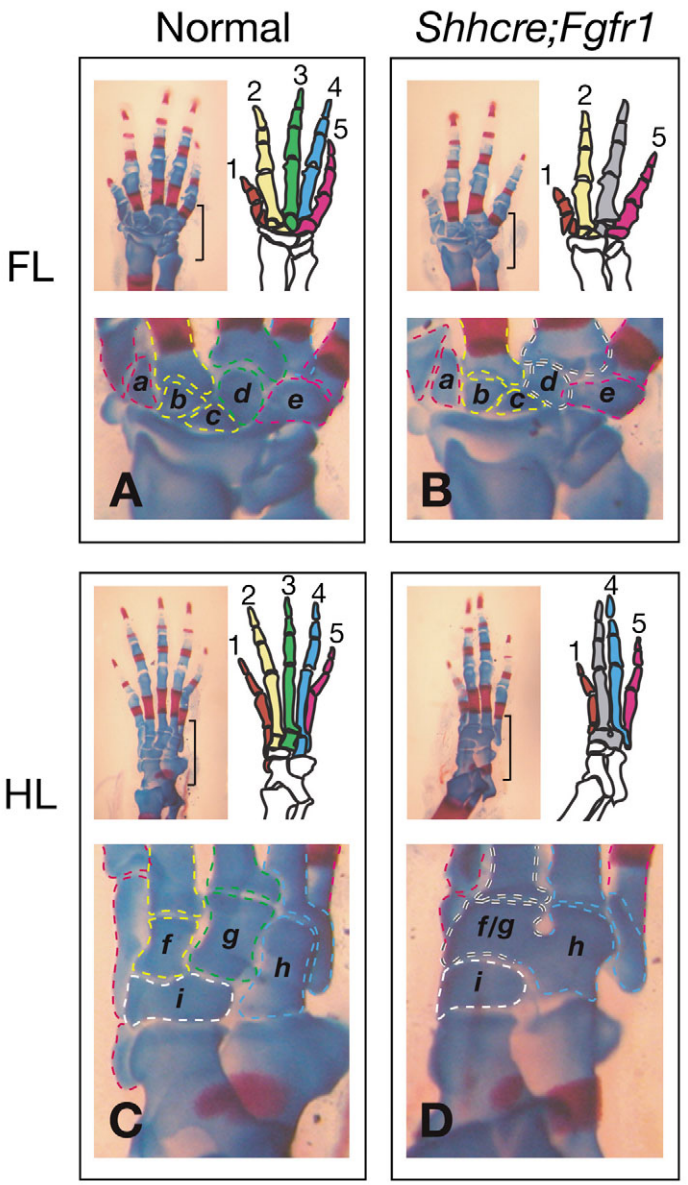

Fig. 6. *Shhcre;Fgfr1* autopod skeletal phenotype. Autopod skeletons of E18.5 embryos demonstrate consistent patterns that are observed in wild-type (n=4) and mutant (n=6) embryos. Shown within each box are a skeletal preparation of an E18.5 autopod (top left panel), a diagram outlining all elements (top right panel) and a magnified view of the wrist region (lower panel). Brackets indicate regions magnified in lower panels. In a normal autopod, individual digits are numbered and colored differentially. In the mutant, each identifiable digit is assigned the number and color of the corresponding normal digit, while the non-identifiable digits are colored grey. In the magnified views, carpal elements relevant to the identification of digits are labeled with letters: a, trapezium; b, trapezoid; c, central carpal; d, capitate; e, hamate; f, intermediate cuneiform; g, lateral cuneiform; h, cuboid; i, navicular. The metacarpals/metatarsals and carpals/tarsals are outlined with broken lines to delineate the connections between them. In both mutant forelimb and hindlimb, digits 1 and 5 are easily identifiable based on their phalanx number, digit length and their metacarpal/metatarsal articulation with the carpals/tarsals. Digit 2 is identified in the mutant forelimb based on its length (shorter than digits 3, 4 and longer than 1, 5), and more importantly on its metacarpal articulation with both the trapezoid (b) and central carpal (c). The grey digit in the mutant forelimb is either a digit 3, 4 or a chimeric 3/4 based on its length (longest of all) and its articulation with both the capitate (d) and the hamate (e). Digit 4 is identified in the mutant hindlimb based on its articulation with the Cuboid (h). The grey digit in the mutant hindlimb is either a digit 2, 3 or a chimeric 2/3 as it articulates with the fused intermediate/lateral cuneiform (f/g) atop the navicular (i). FL, forelimb; HL hindlimb.

(Fig. 7C). In a *Shhcre;Fgfr1* forelimb bud at the same stage, morphology as well as position of the four condensations indicate that digits 1, 2, 4 and 5 condensations are present, while digit 3 condensation is not (Fig. 7D). Examination of E18.5 skeletal preparations show that all mutants analyzed exhibit the same phenotype (n=6 skeletons). Based on phalanx number/shape, digit length and most definitively articulation between metacarpals/metatarsals and carpals/tarsal, we determined that digits 1, 2 and 5 are present in the forelimb (Fig. 6A,B) and digits 1, 4 and 5 are present in the hindlimb (Fig. 6C,D). Thus, the combined evidence is consistent with the conclusion that digit 3 is absent in *Shhcre;Fgfr1* mutant limbs.

Inactivating *Fgfr1* affects *Shh* lineage

The deduction that digit 3 is absent in *Shhcre;Fgfr1* mutant led us to investigate the mechanism behind this defect. Two recent studies proposed that the *Shh*-expressing cell lineage and the SHH-responsive cell lineage are important for the identities of digits 2-5 (Ahn and Joyner, 2004; Harfe et al., 2004). In particular, digit 3 forms at the anterior boundary of the *Shh*-expressing lineage, and is proposed to require the participation of *Shh*-expressing cells, as well as the influence of secreted SHH signaling (Harfe et al., 2004). We found that a change in the *Shh*-expressing lineage may account for the digit defect in the *Shhcre;Fgfr1* mutant.

In an E11.75 forelimb bud comparing β-gal staining and *Sox9* expression at an equivalent stage, the *Shh*-expressing lineage spans two and one-half digits, similar to wild type (Fig. 7E,F). However, the percentage of *lacZ*-expressing cells within the anterior portion of the lineage domain is significantly reduced in the mutant compared with normal. The cause of this reduction is not clear as neither cell death nor cell proliferation differences were detected (data not shown). The lineage reduction phenotype is confirmed at E12.5 when digits are apparent (Fig. 7G,H). Based on the hypothesized cellular and molecular requirements for digit identities (Harfe et al., 2004), we propose that at the anterior boundary of the *Shh*-expressing lineage in the *Shhcre;Fgfr1* limb buds, a reduction in lineage contribution results in a local environment sufficient for the formation of digit 2 but not digit 3.

Discussion

In this study, we generated two mutants in which *Fgfr1* is inactivated in a different temporal and spatial manner. Analyses of these mutants reveal multiple aspects of FGFR1 function in limb outgrowth and patterning (Fig. 8).

Mechanism of FGFR1 function in limb development

The combined data from *Tcre;Fgfr1* and *Shhcre;Fgfr1* mutants lead us to propose that signaling through FGFR1

impacts limb skeletal formation in three phases (Fig. 8). In the early phase, FGFR1 is required for elongating the nascent limb bud along the PD axis and restricting it along the other two axes. In the middle phase, FGFR1 is required for mesenchymal cell survival. In the late phase, FGFR1 is required for autopod patterning by influencing digit placement and identity. The skeletal defect in *Tcre;Fgfr1* mutant is probably due to a combined cellular deficiency in all three phases of limb development, while loss of one digit in *Shhcre;Fgfr1* limbs is due to lack of FGFR1 function in the late phase.

At the molecular level, the reduced expression of several key patterning molecules, including *Shh*, *Hoxa13* and *Hoxd13*, in the two mutants may explain their zeugopod and autopod defects. Certain *Hoxa13;d13* homozygous/heterozygous combination mutants exhibit reduction of digit number and size, similar to that of *Tcre;Fgfr1* mutant (Fromental-Ramain et al., 1996). Although not fully characterized, it is worth noting that the *Tcre;Fgfr1* hindlimb skeletal phenotype closely resembles that of the $Shh^{-/-}$ mutant hindlimb (Fig. 2D) (Chiang et al., 2001; Kraus et al., 2001). As *Shh* expression is drastically reduced in the *Tcre;Fgfr1* hindlimb buds (data not show), the phenotypic similarity is suggestive of a causal relationship. Furthermore, as discussed in more detail below, the lack of digit 3 in *Shhcre;Fgfr1* mutant is probably due to the reduction of *Shh* expression in these limb buds. We note that *Tcre;Fgfr1* mutant exhibits stylopod reduction that is not observed in either $Shh^{-/-}$ or *5′-Hox* mutants. This suggests that there are additional factors mediating FGFR1 function.

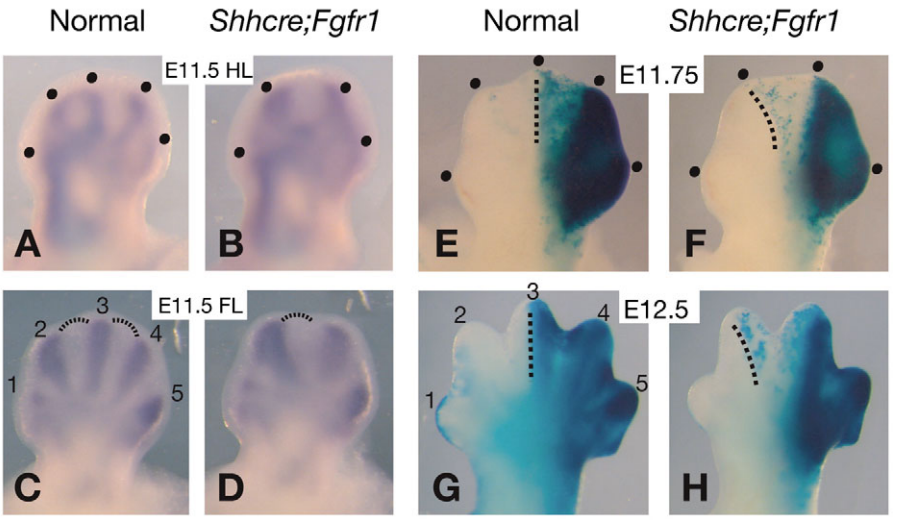

Fig. 7. *Shhcre;Fgfr1* digit condensation and *Shh*-expressing cell lineage. In all panels, anterior is towards the left and posterior towards the right. (A-D) Digit condensations outlined by *Sox9* expression. Dots in A and B indicate individual digit condensations that are beginning to separate. All curved lines in C and D are the same length. All lines are the same length. The lines in C span the entire distance between each pair of condensations, while the line in D does not, indicating that the middle two condensations in D are farther apart than normal. Pattern in C indicates that each condensation has its unique morphology. In particular, digit 2 and 4 condensations have a slight curve towards the straight digit 3 condensation at the midline of the AP axis. In D, the middle two condensations exhibit a curve towards the AP midline, resembling digit 2 and 4 condensations in a normal limb bud. (E-H) β-Gal staining to label *Shh*-expressing cell lineage in normal ($Shh^{cre/+}$;$Fgfr1^{co/+}$;*R26R/+*) and *Shhcre;Fgfr1* ($Shh^{cre/+}$;$Fgfr1^{co/co}$;*R26R/+*) forelimb buds. Dots in E and F indicate the position of condensations as deduced from *Sox9* expression in an equivalent staged limb bud. Broken lines in E-H indicate anterior boundary of the *Shh*-expressing lineage.

FGFR1 restricts cell number and influences the dimensions of a nascent limb bud

The earliest role of FGFR1 in limb bud development is revealed by our analyses of *Tcre;Fgfr1* mutant limb buds. These limb buds initiate normally, but shortly afterwards are misshapen and contain an increased number of cells. Using phosphorylated-Histone staining, we failed to detect any difference in cell proliferation that would account for the cell number increase, although it should be stated that this or any other available methods to detect cell proliferation differences are limited in sensitivity. An alternative explanation for both cell number and limb bud shape defects is that FGFR1

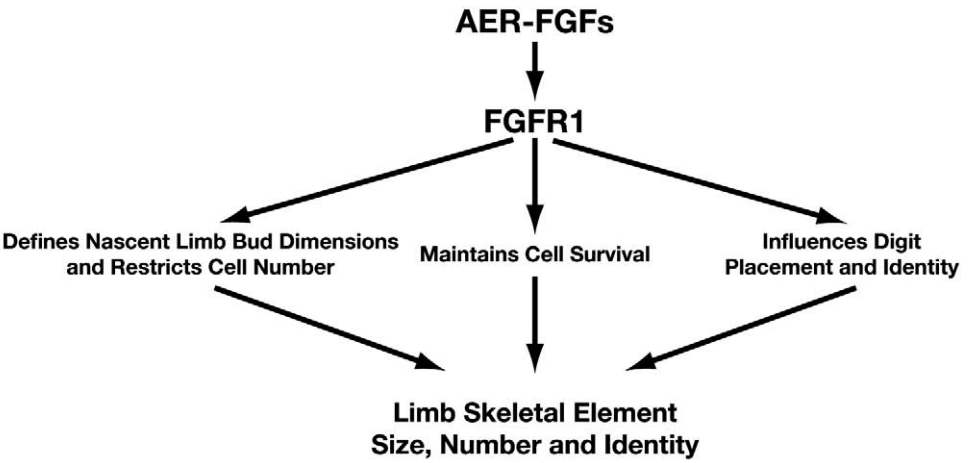

Fig. 8. Mechanism of FGFR1 function. Based on data presented here, we propose that in limb development, FGFR1 serves as a principle receptor for AER-FGF signaling. Activation of FGFR1 then impacts limb skeletal formation through three distinct cellular mechanisms. As elaborated in the Discussion, FGFR1 regulation of *Shh* and *5′-Hox* gene expression probably contributes to the molecular mechanism underlying FGF function during limb bud development.

signaling serves as a permissive cue for changes in cell adhesion, so that only a selected LPM population constitutes a limb bud with set dimensions. This hypothesis is put forth based on previous evidence that FGFR1 influences cell adhesion properties during gastrulation and limb bud formation (Ciruna and Rossant, 2001; Ciruna et al., 1997; Deng et al., 1997; Saxton et al., 2000). For example, in ES cell-derived chimera embryos, it was observed that *Fgfr1*$^{-/-}$ cells accumulate at the base of the limb bud while wild-type cells advance into the distal bud. At first glance, this predicts there would be fewer cells in *Tcre;Fgfr1* nascent limb buds, in contrast to our observation. However, it should be noted that in *Tcre;Fgfr1* embryos, all LPM cells in the vicinity of the prospective limb bud region are mutant for *Fgfr1*, unlike the situation in the ES-cell chimera where mutant cells intermingle with wild-type cells. When all LPM cells are equally compromised in adhesion strength, it is conceivable that by way of stochastic competition more cells from a wider region of the LPM would enter the limb bud. A similar scenario has been documented regarding FGFR1 function in notochord formation. ES cell chimera embryos composed of *Fgfr1* mutant and wild-type cells show that the *Fgfr1*$^{-/-}$ cells are underrepresented in the chimeric notochord (Ciruna et al., 1997). Counterintuitively, a clearly expanded notochord is observed in the *Fgfr1*-null mutant (Deng et al., 1994; Yamaguchi et al., 1994). These seemingly contradictory data present a challenge to understand the precise cellular and molecular mechanisms underlying limb bud establishment. We found here that FGFR1 functions in this process to promote limb PD outgrowth, while restricting the dimensions of the other two axes. In addition, it serves an unexpected role in limiting cell number in a nascent limb bud.

Fgfr1 expressed in LBM is essential for cell survival

Similar excess cell death phenotypes are observed in *Tcre;Fgfr1* mutant and in *AER-Fgf* mutants (Boulet et al., 2004; Lewandoski et al., 2000; Sun et al., 2002), suggesting that AER-FGF signaling mediated by FGFR1 is essential for mesenchymal cell survival. In a wild-type limb bud, limited cell death is observed in the proximal mesenchyme (Fig. 3O), in agreement with previous findings (Dawd and Hinchliffe, 1971; Milaire and Rooze, 1983). We hypothesize that these cells die because they are out of the range of AER-FGF signaling. This is supported by several lines of evidence. First, beads soaked in FGF protein can rescue cell death following AER removal, suggesting that FGF can maintain LBM cell survival (Fallon et al., 1994). Second, secreted FGFs exhibit a limited range, possibly as a result of endocytosis and subsequent degradation in lysosomes (Scholpp and Brand, 2004). Third, using phosphorylated-ERK as an indicator of FGF signal activation, it has been shown that only cells in the distal mesenchyme of the limb bud are under the influence of FGF (Corson et al., 2003). This is confirmed by the expression patterns of Spry genes and *Mkp3*, which are transcriptionally regulated by FGF signaling (Eblaghie et al., 2003; Kawakami et al., 2003; Minowada et al., 1999). Consistent with our hypothesis, the expression pattern of *Spry4* complements the observed cell death domain in normal limb buds (compare Fig. 3S with 3O). This limited range of FGF pathway activation is likely due to restricted diffusion of the ligands, as there is no evidence for a high-distal/low-proximal gradient in the expression of *Fgfr1* and *Fgfr2* in LBM cells (Orr-Urtreger et al., 1991; Peters et al., 1992; Yamaguchi et al., 1992).

Based on our hypothesis, we would argue that the increase in proximal cell death observed in *Tcre;Fgfr1* and *AER-Fgf* mutant limb buds is due to reduced FGF reception and reduced FGF signaling range, respectively, leading to fewer proximal cells being protected from cell death compared with wild type. This is supported by the reduced domain of *Spry2,4* and *Mkp3* expression in these mutants (Fig. 3T; X.S., unpublished). Despite reduction, these indicators of FGF signaling are still expressed in the distal mesenchymal cells of *Tcre;Fgfr1* limb buds (Fig. 3T; data not shown). This may explain why cell death in *Tcre;Fgfr1* limb buds is not detected in the distal mesenchyme, unlike the situation following AER removal (Dudley et al., 2002; Rowe et al., 1982). We speculate that excess cell death in the *Tcre;Fgfr1* limb buds contributes to the later reduction of limb skeleton, in particular the proximal elements.

FGFR1 influences digit number and identity

In both *Tcre;Fgfr1* and *Shhcre;Fgfr1* mutants, digit(s) are missing. However, we propose that the mechanism leading to the loss of digits is different in the two mutants. In the *Tcre;Fgfr1* mutant, a reduction in progenitor cell number is probably the main cause, as evidenced by reduced limb bud size prior to digit condensation (Fig. 4). By contrast, in the *Shhcre;Fgfr1* mutant, limb bud size remains normal when only four instead of five digit condensations are observed (Fig. 7A,B). This suggests that FGFR1 influences the selection of cells from the mesenchyme that constitute digit condensations.

We propose that this influence is achieved through FGFR1 regulation of *Shh* expression. In the *Shhcre;Fgfr1* mutant, the observed downregulation of *Shh* RNA level would presumably result in reduced SHH production. It has been shown that a reduction in SHH production/distribution leads to loss of digits (Lewis et al., 2001).

We propose that at a later stage, FGFR1 also influences the determination of digit identity by regulating *Shh* expression. Recent studies of *Shh*-expressing and SHH-responsive cell lineages suggest that these are key parameters in the hypothesized rules of digit determination (Ahn and Joyner, 2004; Harfe et al., 2004). As discussed at the end of the Results section, based on these rules, the observed reduction of *Shh*-expressing lineage in *Shhcre;Fgfr1* limb buds may be responsible for the failure to form a normal digit 3 in this mutant.

Fgfr1 is required for the expression of key genes in limb bud patterning

The *Shhcre;Fgfr1* mutant is the first mutant in the FGF signaling pathway that offers a rigorous setting to test FGF regulation of gene expression during limb development. We report unequivocal evidence that FGF signaling regulates *Shh* at the RNA level, providing genetic support for the *Fgf/Shh* feedback loop (Laufer et al., 1994; Niswander et al., 1994). In addition, this mutant yields new data on whether FGFR1 regulates gene expression in a cell-autonomous manner. For example, as it was shown that SHH regulates the expression of Bmp genes (Laufer et al., 1994; Yang et al., 1997), it is reasonable to hypothesize that FGFR1 regulates *Bmp4* expression non cell-autonomously through the regulation of

Shh by FGFR1. However, in *Shhcre;Fgfr1* limb buds, the sharp boundary between *Bmp4*-expressing and non-expressing cells corresponds well with the anterior boundary of *Fgfr1* inactivation (arrows in Fig. 5H,J), suggesting that FGFR1 cell-autonomously regulates *Bmp4* expression, instead of acting through secreted SHH.

The effectiveness of using *Shhcre;Fgfr1* limb buds to assay gene expression is also demonstrated by our expression analysis of the paralogous group *Hoxa13* and *Hoxd13*. Both genes are downregulated in *Tcre;Fgfr1* limb buds (Fig. 4I-L), while only *Hoxd13* is downregulated in *Shhcre;Fgfr1* limb buds (Fig. 5L; data not shown). One possible explanation for this difference is that *Fgfr1* may regulate *Hoxd13* cell-autonomously and *Hoxa13* non-cell-autonomously. Thus, the effect on *Hoxa13* gene expression is evident only when *Fgfr1* is inactivated in a larger domain in *Tcre;Fgfr1* limb buds. Alternatively, *Hoxa13* downregulation in *Tcre;Fgfr1* limb buds could be largely due to reduction of the distal mesenchymal cell population that normally expresses *Hoxa13*. The combined gene expression data demonstrate that novel insights can be gained by revisiting FGF regulation of gene expression in *Shhcre;Fgfr1* limb buds. As discussed above, *Shh* and 5′-Hox genes can mediate only a subset of FGFR1 function in limb skeleton formation. Our goal in the near future is to use *Shhcre;Fgfr1* limb buds as a unique setting to identify other candidate mediators of FGF function in limb development.

We thank Dr Chuxia Deng and his laboratory for sharing unpublished information and helpful comments. We are grateful to Dr John Fallon, his laboratory and members of the Sun laboratory for insightful discussions and critical reading of the manuscript. We thank Dr Cliff Tabin for sharing unpublished data on *Shh* expression level in the limb bud. We are grateful to Drs. D. Duboule, R. Harland, N. Itoh, S. Keyse, V. Lefebvre, R. Maxson, A. McMahon, V. Papaioannou, M. Scott and R. Wisdom for providing plasmids from which RNA in situ probes were prepared. We are very grateful to Amber Rew and Minghui Zhao for excellent technical assistance. J.V. was supported by the NIH funded predoctoral training program in Genetics (5T32GM07133). This work was supported by a March of Dimes Basil O'Connor award 5-FY03-13 (to X.S.) and NIH grant RO1 HD045522 (to X.S.).

Supplementary material

Supplementary material for this article is available at
http://dev.biologists.org/cgi/content/full/132/19/4235/DC1

References

Ahn, S. and Joyner, A. L. (2004). Dynamic changes in the response of cells to positive hedgehog signaling during mouse limb patterning. *Cell* **118**, 505-516.

Boulet, A. M., Moon, A. M., Arenkiel, B. R. and Capecchi, M. R. (2004). The roles of Fgf4 and Fgf8 in limb bud initiation and outgrowth. *Dev. Biol.* **273**, 361-372.

Charite, J., McFadden, D. G. and Olson, E. N. (2000). The bHLH transcription factor dHAND controls Sonic hedgehog expression and establishment of the zone of polarizing activity during limb development. *Development* **127**, 2461-2470.

Chiang, C., Litingtung, Y., Harris, M. P., Simandl, B. K., Li, Y., Beachy, P. A. and Fallon, J. F. (2001). Manifestation of the limb prepattern: limb development in the absence of sonic hedgehog function. *Dev. Biol.* **236**, 421-435.

Ciruna, B. and Rossant, J. (2001). FGF signaling regulates mesoderm cell fate specification and morphogenetic movement at the primitive streak. *Dev. Cell* **1**, 37-49.

Ciruna, B. G., Schwartz, L., Harpal, K., Yamaguchi, T. P. and Rossant, J. (1997). Chimeric analysis of fibroblast growth factor receptor-1 (Fgfr1) function: a role for FGFR1 in morphogenetic movement through the primitive streak. *Development* **124**, 2829-2841.

Clements, D., Taylor, H. C., Herrmann, B. G. and Stott, D. (1996). Distinct regulatory control of the Brachyury gene in axial and non-axial mesoderm suggests separation of mesoderm lineages early in mouse gastrulation. *Mech. Dev.* **56**, 139-149.

Corson, L. B., Yamanaka, Y., Lai, K. M. and Rossant, J. (2003). Spatial and temporal patterns of ERK signaling during mouse embryogenesis. *Development* **130**, 4527-4537.

Dawd, D. S. and Hinchliffe, J. R. (1971). Cell death in the "opaque patch" in the central mesenchyme of the developing chick limb: a cytological, cytochemical and electron microscopic analysis. *J. Embryol. Exp. Morphol.* **26**, 401-424.

Deng, C., Bedford, M., Li, C., Xu, X., Yang, X., Dunmore, J. and Leder, P. (1997). Fibroblast growth factor receptor-1 (FGFR-1) is essential for normal neural tube and limb development. *Dev. Biol.* **185**, 42-54.

Deng, C. X., Wynshaw-Boris, A., Shen, M. M., Daugherty, C., Ornitz, D. M. and Leder, P. (1994). Murine FGFR-1 is required for early postimplantation growth and axial organization. *Genes Dev.* **8**, 3045-3057.

Dudley, A. T., Ros, M. A. and Tabin, C. J. (2002). A re-examination of proximodistal patterning during vertebrate limb development. *Nature* **418**, 539-544.

Eblaghie, M. C., Lunn, J. S., Dickinson, R. J., Munsterberg, A. E., Sanz-Ezquerro, J. J., Farrell, E. R., Mathers, J., Keyse, S. M., Storey, K. and Tickle, C. (2003). Negative feedback regulation of FGF signaling levels by Pyst1/MKP3 in chick embryos. *Curr. Biol.* **13**, 1009-1018.

Eswarakumar, V. P., Monsonego-Ornan, E., Pines, M., Antonopoulou, I., Morriss-Kay, G. M. and Lonai, P. (2002). The IIIc alternative of Fgfr2 is a positive regulator of bone formation. *Development* **129**, 3783-3793.

Fallon, J. F., Lopez, A., Ros, M. A., Savage, M. P., Olwin, B. B. and Simandl, B. K. (1994). FGF-2: apical ectodermal ridge growth signal for chick limb development. *Science* **264**, 104-107.

Finch, P. W., Cunha, G. R., Rubin, J. S., Wong, J. and Ron, D. (1995). Pattern of keratinocyte growth factor and keratinocyte growth factor receptor expression during mouse fetal development suggests a role in mediating morphogenetic mesenchymal-epithelial interactions. *Dev. Dyn.* **203**, 223-240.

Fromental-Ramain, C., Warot, X., Messadecq, N., LeMeur, M., Dolle, P. and Chambon, P. (1996). Hoxa-13 and Hoxd-13 play a crucial role in the patterning of the limb autopod. *Development* **122**, 2997-3011.

Grotewold, L. and Ruther, U. (2002). The Wnt antagonist Dickkopf-1 is regulated by Bmp signaling and c-Jun and modulates programmed cell death. *EMBO J.* **21**, 966-975.

Harfe, B. D., Scherz, P. J., Nissim, S., Tian, H., McMahon, A. P. and Tabin, C. J. (2004). Evidence for an expansion-based temporal Shh gradient in specifying vertebrate digit identities. The limb bud Shh-Fgf feedback loop is terminated by expansion of former ZPA cells. *Cell* **118**, 517-528.

Itoh, N. and Ornitz, D. M. (2004). Evolution of the Fgf and Fgfr gene families. *Trends Genet.* **20**, 563-569.

Kawakami, Y., Rodriguez-Leon, J., Koth, C. M., Buscher, D., Itoh, T., Raya, A., Ng, J. K., Esteban, C. R., Takahashi, S., Henrique, D. et al. (2003). MKP3 mediates the cellular response to FGF8 signalling in the vertebrate limb. *Nat. Cell. Biol.* **5**, 513-519.

Khokha, M. K., Hsu, D., Brunet, L. J., Dionne, M. S. and Harland, R. M. (2003). Gremlin is the BMP antagonist required for maintenance of Shh and Fgf signals during limb patterning. *Nat. Genet.* **34**, 303-307.

Knezevic, V., De Santo, R., Schughart, K., Huffstadt, U., Chiang, C., Mahon, K. A. and Mackem, S. (1997). Hoxd-12 differentially affects preaxial and postaxial chondrogenic branches in the limb and regulates Sonic hedgehog in a positive feedback loop. *Development* **124**, 4523-4536.

Kraus, P., Fraidenraich, D. and Loomis, C. A. (2001). Some distal limb structures develop in mice lacking Sonic hedgehog signaling. *Mech. Dev.* **100**, 45-58.

Laufer, E., Nelson, C. E., Johnson, R. L., Morgan, B. A. and Tabin, C. (1994). Sonic hedgehog and Fgf-4 act through a signaling cascade and feedback loop to integrate growth and patterning of the developing limb bud. *Cell* **79**, 993-1003.

Lewandoski, M., Sun, X. and Martin, G. R. (2000). Fgf8 signalling from the AER is essential for normal limb development. *Nat. Genet.* **26**, 460-463.

Lewis, P. M., Dunn, M. P., McMahon, J. A., Logan, M., Martin, J. F., St-Jacques, B. and McMahon, A. P. (2001). Cholesterol modification of sonic hedgehog is required for long-range signaling activity and effective modulation of signaling by Ptc1. *Cell* **105**, 599-612.

Michos, O., Panman, L., Vintersten, K., Beier, K., Zeller, R. and Zuniga, A. (2004). Gremlin-mediated BMP antagonism induces the epithelial-mesenchymal feedback signaling controlling metanephric kidney and limb organogenesis. *Development* **131**, 3401-3410.

Milaire, J. and Rooze, M. (1983). Hereditary and induced modifications of the normal necrotic patterns in the developing limb buds of the rat and mouse: facts and hypotheses. *Arch. Biol. (Bruxelles)* **94**, 459-490.

Min, H., Danilenko, D. M., Scully, S. A., Bolon, B., Ring, B. D., Tarpley, J. E., DeRose, M. and Simonet, W. S. (1998). Fgf-10 is required for both limb and lung development and exhibits striking functional similarity to Drosophila branchless. *Genes Dev.* **12**, 3156-3161.

Minowada, G., Jarvis, L. A., Chi, C. L., Neubuser, A., Sun, X., Hacohen, N., Krasnow, M. A. and Martin, G. R. (1999). Vertebrate Sprouty genes are induced by FGF signaling and can cause chondrodysplasia when overexpressed. *Development* **126**, 4465-4475.

Mukhopadhyay, M., Shtrom, S., Rodriguez-Esteban, C., Chen, L., Tsukui, T., Gomer, L., Dorward, D. W., Glinka, A., Grinberg, A., Huang, S. P. et al. (2001). Dickkopf1 is required for embryonic head induction and limb morphogenesis in the mouse. *Dev. Cell* **1**, 423-434.

Neubuser, A., Peters, H., Balling, R. and Martin, G. R. (1997). Antagonistic interactions between FGF and BMP signaling pathways: a mechanism for positioning the sites of tooth formation. *Cell* **90**, 247-255.

Niswander, L. (2003). Pattern formation: old models out on a limb. *Nat. Rev. Genet.* **4**, 131-141.

Niswander, L., Jeffrey, S., Martin, G. R. and Tickle, C. (1994). A positive feedback loop coordinates growth and patterning in the vertebrate limb. *Nature* **371**, 609-612.

Ohuchi, H., Nakagawa, T., Yamamoto, A., Araga, A., Ohata, T., Ishimaru, Y., Yoshioka, H., Kuwana, T., Nohno, T., Yamasaki, M. et al. (1997). The mesenchymal factor, FGF10, initiates and maintains the outgrowth of the chick limb bud through interaction with FGF8, an apical ectodermal factor. *Development* **124**, 2235-2244.

Ornitz, D. M., Xu, J., Colvin, J. S., McEwen, D. G., MacArthur, C. A., Coulier, F., Gao, G. and Goldfarb, M. (1996). Receptor specificity of the fibroblast growth factor family. *J. Biol. Chem.* **271**, 15292-15297.

Orr-Urtreger, A., Givol, D., Yayon, A., Yarden, Y. and Lonai, P. (1991). Developmental expression of two murine fibroblast growth factor receptors, flg and bek. *Development* **113**, 1419-1434.

Orr-Urtreger, A., Bedford, M. T., Burakova, T., Arman, E., Zimmer, Y., Yayon, A., Givol, D. and Lonai, P. (1993). Developmental localization of the splicing alternatives of fibroblast growth factor receptor-2 (FGFR2). *Dev. Biol.* **158**, 475-486.

Partanen, J., Schwartz, L. and Rossant, J. (1998). Opposite phenotypes of hypomorphic and Y766 phosphorylation site mutations reveal a function for Fgfr1 in anteroposterior patterning of mouse embryos. *Genes Dev.* **12**, 2332-2344.

Perantoni, A. O., Timofeeva, O., Naillat, F., Richman, C., Pajni-Underwood, S., Wilson, C., Vainio, S., Dove, L. F. and Lewandoski, M. (2005). Inactivation of FGF8 in early mesoderm reveals an essential role in kidney development. *Development* **132**, 3859-3871.

Peters, K. G., Werner, S., Chen, G. and Williams, L. T. (1992). Two FGF receptor genes are differentially expressed in epithelial and mesenchymal tissues during limb formation and organogenesis in the mouse. *Development* **114**, 233-243.

Revest, J. M., Spencer-Dene, B., Kerr, K., De Moerlooze, L., Rosewell, I. and Dickson, C. (2001). Fibroblast growth factor receptor 2-IIIb acts upstream of Shh and Fgf4 and is required for limb bud maintenance but not for the induction of Fgf8, Fgf10, Msx1, or Bmp4. *Dev. Biol.* **231**, 47-62.

Ros, M. A., Dahn, R. D., Fernandez-Teran, M., Rashka, K., Caruccio, N. C., Hasso, S. M., Bitgood, J. J., Lancman, J. J. and Fallon, J. F. (2003). The chick oligozeugodactyly (ozd) mutant lacks sonic hedgehog function in the limb. *Development* **130**, 527-537.

Rowe, D. A., Cairns, J. M. and Fallon, J. F. (1982). Spatial and temporal patterns of cell death in limb bud mesoderm after apical ectodermal ridge removal. *Dev. Biol.* **93**, 83-91.

Saxton, T. M., Ciruna, B. G., Holmyard, D., Kulkarni, S., Harpal, K., Rossant, J. and Pawson, T. (2000). The SH2 tyrosine phosphatase Shp2 is required for mammalian limb development. *Nat. Genet.* **24**, 420-423.

Scholpp, S. and Brand, M. (2004). Endocytosis controls spreading and effective signaling range of Fgf8 protein. *Curr. Biol.* **14**, 1834-1841.

Sekine, K., Ohuchi, H., Fujiwara, M., Yamasaki, M., Yoshizawa, T., Sato, T., Yagishita, N., Matsui, D., Koga, Y., Itoh, N. et al. (1999). Fgf10 is essential for limb and lung formation. *Nat. Genet.* **21**, 138-141.

Soriano, P. (1999). Generalized lacZ expression with the ROSA26 Cre reporter strain. *Nat. Genet.* **21**, 70-71.

Sun, X., Mariani, F. V. and Martin, G. R. (2002). Functions of FGF signalling from the apical ectodermal ridge in limb development. *Nature* **418**, 501-508.

Takahashi, M., Tamura, K., Buscher, D., Masuya, H., Yonei-Tamura, S., Matsumoto, K., Naitoh-Matsuo, M., Takeuchi, J., Ogura, K., Shiroishi, T. et al. (1998). The role of Alx-4 in the establishment of anteroposterior polarity during vertebrate limb development. *Development* **125**, 4417-4425.

Xu, X., Weinstein, M., Li, C., Naski, M., Cohen, R. I., Ornitz, D. M., Leder, P. and Deng, C. (1998). Fibroblast growth factor receptor 2 (FGFR2)-mediated reciprocal regulation loop between FGF8 and FGF10 is essential for limb induction. *Development* **125**, 753-765.

Xu, X., Li, C., Takahashi, K., Slavkin, H. C., Shum, L. and Deng, C. X. (1999). Murine fibroblast growth factor receptor 1alpha isoforms mediate node regression and are essential for posterior mesoderm development. *Dev. Biol.* **208**, 293-306.

Xu, X., Qiao, W., Li, C. and Deng, C. X. (2002). Generation of Fgfr1 conditional knockout mice. *Genesis* **32**, 85-86.

Yamaguchi, T. P., Conlon, R. A. and Rossant, J. (1992). Expression of the fibroblast growth factor receptor FGFR-1/flg during gastrulation and segmentation in the mouse embryo. *Dev. Biol.* **152**, 75-88.

Yamaguchi, T. P., Harpal, K., Henkemeyer, M. and Rossant, J. (1994). fgfr-1 is required for embryonic growth and mesodermal patterning during mouse gastrulation. *Genes Dev.* **8**, 3032-3044.

Yang, Y., Drossopoulou, G., Chuang, P. T., Duprez, D., Marti, E., Bumcrot, D., Vargesson, N., Clarke, J., Niswander, L., McMahon, A. et al. (1997). Relationship between dose, distance and time in Sonic Hedgehog-mediated regulation of anteroposterior polarity in the chick limb. *Development* **124**, 4393-4404.

Yu, K., Xu, J., Liu, Z., Sosic, D., Shao, J., Olson, E. N., Towler, D. A. and Ornitz, D. M. (2003). Conditional inactivation of FGF receptor 2 reveals an essential role for FGF signaling in the regulation of osteoblast function and bone growth. *Development* **130**, 3063-3074.

Zakany, J., Fromental-Ramain, C., Warot, X. and Duboule, D. (1997). Regulation of number and size of digits by posterior Hox genes: a dose-dependent mechanism with potential evolutionary implications. *Proc. Natl. Acad. Sci. USA* **94**, 13695-13700.

Zucker, R. M., Hunter, E. S., 3rd and Rogers, J. M. (1999). Apoptosis and morphology in mouse embryos by confocal laser scanning microscopy. *Methods* **18**, 473-480.

Table S1. Total cell number in *Tcre;Fgfr1* mutant forelimb buds compared with normal control

	Tcre;Fgfr1	Normal	% change
E10.0	$9.9\pm0.53\times10^4$ (n=4)	$6.0\pm1.5\times10^4$ (n=6)	+65
E10.5	$2.5\pm0.31\times10^5$ (n=6)	$1.9\pm0.21\times10^5$ (n=6)	+31
E11.5	$3.2\pm0.22\times10^5$ (n=6)	$4.2\pm0.32\times10^5$ (n=6)	–26

The number (n) of single limb buds assayed for each genotype and stage is indicated. Embryos were dissected in Ca^{2+}/Mg^{2+}-free (CMF)-PBS and washed three times. Individual limb buds were incubated in 100 µl CMF-PBS for 30 minutes at 37°C. After incubation the ectoderm was peeled away from the mesenchyme. The mesenchyme was then dissociated by incubating in 100 µl of 0.5% trypsin (Invitrogen) with 1% pancreatin (Sigma) at 4°C for 20 minutes followed by 15 minutes at 37°C. After incubation 50 µl of fetal bovine serum (FBS) was added to the mixture. Limb bud pieces were collected by centrifuging at 3000 rpm for 30 seconds and washed three times each in 200 µl of DMEM with 10% FBS. After the final wash, 100 µl of DMEM was added and the limb bud was titurated until all tissue clumps disappeared. After centrifugation the pelleted cells were resuspended in 50 µl of DMEM and counted using a hemocytometer.